Applied Energy 217 (2018) 496–508

Contents lists available at ScienceDirect

Applied Energy

journal homepage: www.elsevier.com/locate/apenergy

A conceptual study on air jet-induced swirling plume for performance improvement of natural draft cooling towers

Yuanshen Lu[a,*], Alexander Klimenko[a], Hugh Russell[a], Yuchen Dai[a], John Warner[b], Kamel Hooman[a]

[a] School of Mechanical and Mining Engineering, The University of Queensland, Qld 4072, Australia
[b] Jord International, Sydney, NSW, Australia

HIGHLIGHTS

- The new concept of swirling plume significantly enhances cooling capacity of NDCTs.
- The cooling enhancement recovers power cycle output at high ambient temperature.
- The swirling plume creates an equivalent extra draft height above the tower.
- Air jet speed, direction, and nozzle size are the key controlling parameters.
- The concept consumes lower power than fan-forced coolers in long-term operations.

ARTICLE INFO

Keywords:
Natural draft cooling towers
Vortex cooling tower
Cooling enhancement
Swirling plume
Updraft vortex
Power cycle efficiency

ABSTRACT

In thermal power cycles including concentrating solar thermal (CST) plants, natural draft cooling towers (NDCTs) are widely used heat-dumping facilities. One inherent drawback of NDCTs is that their cooling performance can be compromised by changes in ambient conditions, particularly temperature, which inevitably reduces the net power output of the cycles. Current methods resolving this issue are limited in a few options including inlet air pre-cooling, exit air heating, and fan assistance, each with considerable operational or initial cost. To more economically reduce energy efficiency losses of the power cycles due to inefficient cooling, this paper proposes a new concept of swirling plume method for both dry- and wet-type NDCTs. The method is to rotate the plume strongly like a tornado in the tower upper part and above the towers to increase the overall tower updraft capacity (pressure). The swirling plume is induced by high-speed air jets distributed at certain locations using a much smaller flow rate. A numerical investigation on a 20 m-tall dry-type NDCT model has been conducted verifying that this concept increases the airflow and the water temperature drop of the heat exchanger by at least 53.6% and 3.57 °C (39.2%), respectively, under 35 °C ambient temperature. This cooling performance enhancement enables a half megawatt-scale sCO_2-based CST power cycle to recover its net power output, by 4.98%, to the level almost same as that at 30 °C ambient temperature. The air jet to create such a swirling plume consumes only 1/7 of the recovered power roughly. Compared with a traditional fan-forced cooler working under exactly the same condition, this concept requires significantly smaller energy in long-term operations as it would run only during temperature extremes. A simplified analytical modelling has found that the cooling tower performance is improved due to that the swirling plume creates an equivalent extra draft height on top of the tower which is attributed to two different vortical effects. The overall angular momentum of the swirl is a critical factor in these effects.

1. Introduction

Natural draft cooling towers (NDCTs) are widely used to remove heat in thermal power plants and many other industrial process. In Concentrated solar thermal (CST) power plants, the redundant heat downstream to turbines is usually removed by these facilities. The heat dump efficiency of the cooling towers is one of the crucial factors affecting the overall power conversion (heat-to-electricity) efficiency of the plants. Furthermore, the parasitic loss of power to run the cooling equipment is an important consideration. While NDCTs have the

* Corresponding author.
E-mail address: yuanshen.lu@uqconnect.edu.au (Y. Lu).

https://doi.org/10.1016/j.apenergy.2018.02.095
Received 12 December 2017; Received in revised form 9 February 2018; Accepted 12 February 2018
Available online 03 March 2018
0306-2619/

Nomenclature

A	area (m^2)
A_{Jn}	effective nozzle area normal to the jet stream, respectively (m^2)
a	jet direction angle (°)
b	jet direction angle (°)
C	inertial resistance factor in porous media
C_p	specific heat ($J\,Kg^{-1}\,K^{-1}$)
C_μ	constant in turbulent viscosity
dn	thickness of porous media zone (m)
H	tower height (m)
h_r	convective heat transfer coefficient of radiator (heat exchangers) ($W\,m^{-2}\,K^{-1}$)
K, K_e, K_t	laminar, effective, turbulent thermal conductivity, respectively ($W\,m^{-1}\,K^{-1}$)
K_{to}	loss coefficient at the tower outlet
K_Σ	total pressure loss coefficient throughout the cooling tower
k	turbulent kinetic energy ($m^2\,s^{-2}$)
m_a	air mass flow rate ($kg\,s^{-1}$)
m_{aJ}	jet air mass flow rate ($kg\,s^{-1}$)
P	pressure (pa)
Pr, Pr_t	laminar, turbulent Prandtl number, respectively
ΔP_r	pressure difference across radiator (heat exchangers) (pa)
ΔP_{Ft}, ΔP_{Fs}	total pressure and static pressure of fan, respectively (pa)
q_r	heat flux of the radiator (heat exchangers) ($W\,m^{-2}$)
R	cooling tower radius (m)
S	volumetric source term
T	temperature (K)
U	velocity component in x-, y-, or z- direction ($m\,s^{-1}$)
V_F	volumic flow rate of fan ($m^3\,s^{-1}$)
v	velocity ($m\,s^{-1}$)
v_a, v_F, v_J	air velocity inside the cooling tower, at fan outlet, and of the jet, respectively ($m\,s^{-1}$)
v_{rJ}, $v_{\theta J}$, v_{zJ}	air jet velocity in radial, tangential and vertical (axial) directions ($m\,s^{-1}$)
W_F, W_J	powers input of fans and jet nozzles, respectively ($J\,s^{-1}$)
r, θ, z	cylindrical system co-ordinates: radial, tangential, and axial (vertical)
x	Cartesian system co-ordinates
z	elevation (m)
i, j, k	Cartesian co-ordinate serial

Greek letters

α	permeability in porous media (m^2) or velocity distribution factor
α^*, $\hat{\alpha}$	constants in pressure-strain tensor
β, β^*, $\hat{\beta}$	constants in pressure-strain tensor
γ^*, $\hat{\gamma}$	constants in pressure-strain tensor
ε	characteristic factor of plume vortex for static pressure
η_θ, η_z	factor of conservation of momentum
η_{Ft}	total efficiency of fan
ρ	density ($kg\,m^{-3}$)
ρ_O, ρ_I	air density outside and inside the cooling tower, respectively ($kg\,m^{-3}$)
μ, μ_e, μ_t	laminar, effective, turbulent viscosity, respectively ($kg\,m^{-1}\,s^{-1}$)
σ_ω, $\sigma_{\omega 2}$	constants in the transport equation of ω
ω	turbulence energy specific dissipation rate (s^{-1})

Vectors

$\hat{\boldsymbol{e}}$	unit moment vector in co-ordinate directions
$\boldsymbol{M}$	momentum vector
$\boldsymbol{v}$	velocity vector

Tensors/matrix

D_{ij}, P_{ij}, S_{ij}	production tensors of Reynolds stresses
δ_{ij}	indentity matrix
ε_{ij}	dissipation tensor
Φ_{ij}	pressure-strain tensor

Subscripts

a	air or air side
E	energy
e	effective
F	fans
I, O	inside or inlet, outside or outlet
J	nozzle jet
M	momentum
r	radiator (heat exchangers)

unbeatable advantage of using no power, one of their drawbacks is that the cooling performance on these towers, especially natural draft dry cooling towers (NDDCTs), is highly compromised by changes in ambient temperatures: the higher the ambient temperatures, the lower the heat transfer rate to atmosphere. Because of this, NDCTs are always expected to be overdesigned to meet the desired cooling load at all time.

However, practical designs of NDCTs in thermal power plants are actually governed by a trade-off between the cooling performance and the capital costs. As the result, they only provide sufficient cooling loads for target ambient temperatures selected based on, for example, the 95th–98th percentile of hourly ambient temperature in a year, not 100%. During the small portion of a year when ambient temperature is higher than the design values, the cooling towers cannot cool down the cooling media sufficiently so that the overall power conversion efficiency drops. In base-load power plants, increasing fuel supply is a very common solution to offset the efficiency loss caused by poor cooling. A better option is to recover the cooling capacity during the periods at a less cost.

Currently, there are a few methods to improve the cooling performance of NDCTs against high ambient temperatures. For dry towers, various evaporation-based approaches have been proposed including dry-wet hybrid cooling [1–4] and inlet air precooling [5–7]. These methods consume large volumes of water, and require accessory water supply systems. They cannot be used in conjunction with wet cooling towers. One type of methods which is applicable to both dry and wet towers is devising a way to increase the temperature of hot air inside cooling towers to increase the air buoyancy so that the air flow rate. This includes heat injection [8] and solar radiation [9] downstream to the heat exchange zones (either heat exchangers or wet fills). Dynamical water distribution adjustment across the plane of heat exchangers to optimise the local heat transfer is also considered a useful method in enhancing both cooling tower types [10,11]. In the cases when crosswind presents, the cooling tower performance may be improved by taking use of the wind through windbreak walls, wind shells, deflectors, or the periphery of a tower base [12–23], which has been intensively studied in the past decade. More directly, air flow in NDCTs can be enhanced by deploying assistant fans at the inlets or above heat exchange zones [24,25]. The method usually chooses options from super-big fans [26], lots of smaller fans [27,28], and less small fans with

transition components to distribute airflow more evenly. However, most industrial fans work at air speeds much higher than those driven by pure natural convection, unless they sacrifice their power efficiency. This causes extra high pressure losses across heat exchangers which are initially designed for significantly lower airflow rate, and thus the overall efficiency of using fans are compromised. More importantly, the moving parts and the supporting structures of fans inevitably introduce additional blockages to original cooling towers.

On the other hand, rotational air flow, or air vortex, has been demonstrated by natural tornados to have the ability of flow augment. Attempts to utilize this effect thus have been made on cooling towers/chimneys through patents such as [29,30], despite lack of actual proof. Hemmasian Kashani et al. [31,32] numerically studied the influence of flow rotation in the over-shower zone of a natural draft wet cooling tower and found that the rotation intensifies heat and mass transfer in the zone [31] and increases the homogeneity of the flow field inside cooling towers under certain crosswind conditions [32]. The authors proposed that the flow rotation could be generated by a type of deflectors, but failed to give any detail. The interest of the discussion was also restricted in the tower internal flow field. Dobrego et al. [33] proposed to introduce a vortex flow of the vapour–air mixture above spray zones in NDWCTs by setting water sprayers at a proper azimuthal orientation. The vortex is believed to increase the operation stability of NDWCTs under medium and large wind loads. However, according to the authors, only a small part (up to 30%) of the water spray momentum can be used to set the swirling vapour–air flow [33] and, more importantly, the exact benefit of the method is still unknown due to the simplicity of the study.

In view of the above, a new concept of swirling plume airflow boost in NDCTs, be it wet or dry, is proposed by the authors. The basic idea is to rotate the plume about the central vertical axis, like a tornado, in the upper part and above the cooling towers by using a number of high speed air jets distributed at certain locations. The tornado-like vortex increases the airflow through the heat transfer zones in lower part of the towers at the cost of a much smaller jet flow rate than that of the main airstream. The jets can be produced by efficient fans/blowers through nozzles embedded in the inner surface of the tower wall at certain orientation angles, and may be sourced from the hot air above the heat exchange or the ambient cool air, as shown in Fig. 1.

The concept differs from the aforementioned existing proposals on that it introduces the flow rotation actively, and adopts a much higher swirling ratio (defined as the ratio of circulation speed to the updraft one) so that it can benefit from “extra bonus”—the increase of updraft force caused by the air vortex. Unlike conventional fan-assisted methods, this concept eliminates visible moving parts and their supporting structures, and thus has no influence to the NDCTs in normal pure natural convection operations. It is ideal for intermittent use to cope with energy conversion efficiency losses of thermal power plants due to diurnal or seasonal changes in ambient temperature.

To the best of our knowledge, proposals similar to the concept of jet-induced swirling plume for natural draft cooling tower enhancement have not been discussed in open literatures yet, neither have the mechanisms of the vortex effect on tower draft force enhancement. In fundamental fluid mechanics, theories connecting buoyant swirling turbulent plume and natural convective updraft effect are still under development and have been seldom applied to practical engineering problems so far.

To fill this gap, a numerical and analytical study on the jet-induced swirling plume in a 20 m-tall NDDCT model has been conducted in this paper. The effectiveness of the proposed concept on cooling tower performance improvement is assessed and verified for the first time. Then, a simplified 1-dimensional model is introduced to preliminarily investigate the flow enhancement mechanisms on the NDDCT with the air jet-induced swirling plume, revealing that there are multiple effects attributed to the flow augment of swirling plume. Results from both the numerical and analytical methods are cross-validated and found to be in good agreement. Following the discussions on the controlling parameters of the swirling plume, the paper estimates the power consumption of air jets and the benefit of the concept on the net power output of a half megawatt-scale sCO_2-based CST power cycle.

2. CFD model setup

The jet-induced swirling plume of a natural draft cooling tower was simulated numerically. A cylindrical natural draft dry cooling tower model with 20 m height and 12 m diameter was set up using the commercial software ANSYS Fluent. The prototype of this model is an actual 20 m-tall steel-membrane cooling tower built in a campus of The University of Queensland for a future small-scale CST power plant using a supercritical CO_2 Brayton cycle [34,35]. The tower body in the CFD model only kept the main features of the prototype while most detailed structures were ignored.

2.1. Models and boundary conditions

The boundary condition and dimensions of the cooling tower model and the whole computational domain are illustrated in Fig. 2. As indicated, eight air jet nozzles were proposed to be distributed evenly on the tower inner wall at the location 10 m above the heat exchangers of the cooling tower. The jet nozzles were modelled by eight curved rectangular faces with velocity inlet boundary conditions. The jet stream velocity were specified through both the magnitude and the direction. The latter was defined by azimuthal angle a and pitching angle b, which was implemented in CFD through specifying radial, tangential, and axial components in a cylindrical coordinate system at the boundaries. The temperature at these boundaries were set to be same as the averaged one right above the heat exchangers, while the static pressure was interpolated during the iterations.

In addition to the jet velocity, a jet area, A_{jn}, was also defined as the nozzle area perpendicular to the jet stream. As the result, the areas of the curved rectangular faces varied from one case to another depending on the jet direction, in order to keep A_{jn} constant at 0.089 m^2, except for Case 8.

In this study, 9 different combination cases of jet magnitude, direction, and area were considered with details as per Table 1 below. These combinations cover the most typical setups in practical applications. Case 0 stands for the normal situation when the cooling tower operates only under pure natural draft mode with no swirling plume. Case 1 represents an arbitrarily selected configuration of the nozzle jets—angle a at 60° and angle b at 30° with the jet speed of 20 m/s. Cases 2–6 explores the effect of jet directions using the exactly same size nozzle (0.089 m^2) at the same speed (20 m/s) in Case 1, among which Cases 2–4 stands for air jets in radial direction only, in axial direction only, and in both radial and tangential directions, respectively. The selection of these cases enabled the determination of how the jet direction influence the overall effect of the swirling plume. The rest two cases (Cases 7 and 8) were used to examine the effect of jet stream flow rate. Specifically, Case 7 differs from Case 1 in only the jet

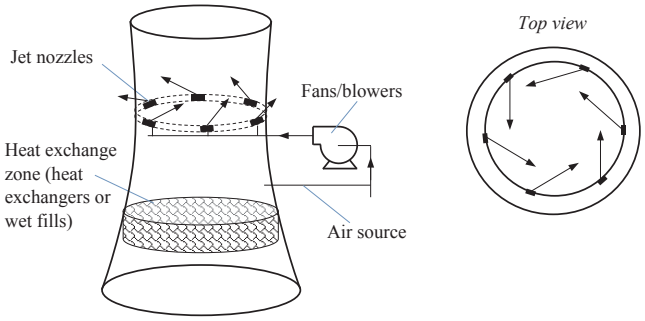

Fig. 1. A schematic of the concept of the air jet-induced plume vortex on NDCTs.

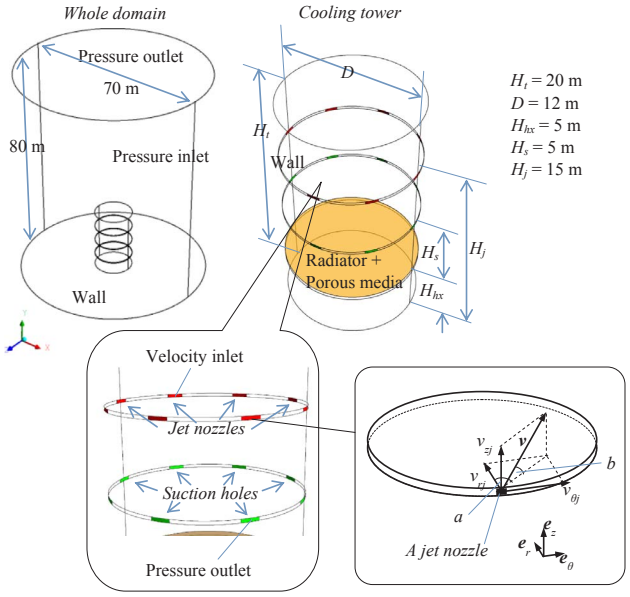

Fig. 2. The boundary conditions in the CFD model.

speed (15 m/s), while Case 8 in only the nozzle size (0.3 m^2).

Each jet nozzle corresponds to a suction hole underneath. The suction holes were modelled as pressure outlet boundaries with an outflow rate same to the one of the jet nozzles. The actual static pressure at the holes was then iteratively computed to match the flowrate.

The heat exchangers were modelled by a uniformly-thick zone treated as a porous media zone with its upper surface set as radiator boundary condition [36,37]. In the porous media zone, an additional source term S_i representing the pressure loss within the heat exchanger is added to the momentum equation. S_i is expressed as

$$S_{Mi} = -\left(\frac{C}{2}\rho v_i^2 + \frac{\mu_e}{\alpha}v_i\right) \Big/ dn \quad (i = 1,2,3) \tag{1}$$

where dn is the thickness of the porous zone. α and C are coefficients which were derived from an empirical pressure drop-air speed correlation provided by the manufacturer of the heat exchangers of the Gatton cooling tower, namely:

$$\Delta P_r = 6.65v_a^2 + 5.205v_a \tag{2}$$

The radiator boundary calculates the heat flux q_r added to the air to representing the heat transfer at heat exchangers [38,39]:

$$q_r = h_r(T_r - T_{ao}) \tag{3}$$

where T_{ao} is the air outlet temperature of the heat exchanger. h_r is the overall heat transfer coefficient which can be estimated by another empirical correlation of the prototype tower [40]:

$$h_r = 150.07v_a^2 + 549.22v_a + 190.95 \tag{4}$$

Inlet and outlet pressure boundaries were applied to the side and the top of the computational domain to define the ambient air condition, where the static pressure and the temperature were specified as zero and 35 °C, respectively.

2.2. Governing equations

The Reynolds decomposed steady-state conservation equations of mass, momentum, and energy for air are given by Eqs. (5)–(7)

$$\frac{\partial}{\partial x_j}(\rho U_j) = 0 \tag{5}$$

$$\frac{\partial(\rho U_j U_i)}{\partial x_j} = -\frac{\partial}{\partial x_i}\left(P + \frac{2}{3}\mu\frac{\partial U_k}{\partial x_k}\right) + \frac{\partial}{\partial x_i}\left[\mu\left(\frac{\partial U_i}{\partial x_j} + \frac{\partial U_j}{\partial x_i}\right) - \rho\overline{u_i u_j}\right] + S_{Mi} \tag{6}$$

$$\frac{\partial}{\partial x_j}[u_i(\rho E + P))] = \frac{\partial}{\partial x_j}\left[\left(k + \frac{C_p\mu_t}{Pr_t}\right)\frac{\partial T}{\partial x_j}\right] + \frac{\partial}{\partial x_j}\left\{U_i\left[\mu_e\left(\frac{\partial U_i}{\partial x_j} + \frac{\partial U_j}{\partial x_i}\right) - \rho\overline{u_i u_j}\right]\right\} + S_{Ei} \tag{7}$$

where $\rho\overline{u_i u_j}$ represents the averaged fluctuating turbulence stresses, Reynolds stresses. Here, i,j,k = 1,2,3. E is the total energy and μ_e is the effective viscosity which is the sum of the molecular and turbulent viscosities, i.e. $\mu_e = \mu + \mu_t$. Reynolds stresses are second order tensors composed of 9 unknown components, which need to be modelled to close Eqs. (5)–(7).

Because of the anisotropic nature of the swirling turbulence, a higher order turbulence model—Reynolds Stress model is preferred [41]. Effectively, a separate transport Eq. (8) must be solved for each of the Reynolds stress components. Since the air in this modelling is assumed as incompressible Newtonian fluid, only six out of the 9 components are actually independent and need to be solved, namely $\rho\overline{uu}$, $\rho\overline{vv}$, $\rho\overline{ww}$, $\rho\overline{uv}$, $\rho\overline{uw}$, and $\rho\overline{vw}$.

$$\frac{\partial}{\partial x_k}(U_k\rho\overline{u_i u_j}) = \frac{\partial}{\partial x_k}\left[\left(\frac{\mu_t}{\sigma_k} + \mu\right)\frac{\partial\overline{u_i u_j}}{\partial x_k}\right] - \left(\overline{\rho u_i u_k}\frac{\partial U_j}{\partial x_k} + \overline{\rho u_j u_k}\frac{\partial U_i}{\partial x_k}\right) + \Phi_{ij} - \varepsilon_{ij} \tag{8}$$

In the above equation, the pressure-strain tensor Φ_{ij}, and the dissipation tensor ε_{ij} need to be modelled using the expressions below:

$$\Phi_{ij} = -C_1\beta^*\rho\omega\left(-\overline{u_i u_j} + \frac{2}{3}k\delta_{ij}\right) - \hat{\alpha}\left(P_{ij} - \frac{1}{3}P_{kk}\delta_{ij}\right) - \hat{\beta}\left(D_{ij} - \frac{1}{3}P_{kk}\delta_{ij}\right) - \hat{\gamma}\rho k\left(S_{ij} - \frac{1}{3}S_{kk}\delta_{ij}\right) \tag{9}$$

$$\varepsilon_{ij} = \frac{2}{3}\delta_{ij}\rho\beta^* k\omega \tag{10}$$

where the three additional tensors are defined as $P_{ij} = -\overline{\rho u_i u_k}\frac{\partial U_j}{\partial x_k} - \overline{\rho u_j u_k}\frac{\partial U_i}{\partial x_k}$, $D_{ij} = -\overline{\rho u_i u_k}\frac{\partial U_k}{\partial x_j} - \overline{\rho u_j u_k}\frac{\partial U_k}{\partial x_i}$ and $S_{ij} = \frac{1}{2}(\frac{\partial U_j}{\partial x_i} + \frac{\partial U_i}{\partial x_j})$. The turbulent viscosity is $\mu_t = C_\mu\rho\frac{k}{\omega}$, and turbulence kinetic energy is $k = \frac{1}{2}\overline{u_i u_i}$. The constants are $\alpha^* = 1$, $\beta^* = 0.09$, $\hat{\alpha} = 0.775$, $\hat{\beta} = 0.196$, $C_\mu = 0.09$, $\hat{\gamma} = 0.495$, $Pr = 0.74$, and $Pr_t = 0.85$.

The transport equation of Reynolds stresses Eq. (8) involves another unknown quantity ω, turbulent frequency, which requires the equation below to close the whole set of governing equations:

Table 1
Key parameters for the air jet nozzles in all 9 cases for 35 °C ambient temperature.

Parameter	Case 0	Case 1	Case 2	Case 3	Case 4	Case 5	Case 6	Case 7	Case 8
a (°)	N/A	60	0	N/A	60	70	60	60	60
b (°)		30	0	90	0	30	45	30	30
v (m/s)		20	20	20	20	20	20	15	20
A_{jn} (m^2)		0.089							0.3

$$\frac{\partial}{\partial x_j}(U_j\rho\omega) = \frac{\partial}{\partial x_j}\left[\left(\mu + \frac{\mu_t}{\sigma_\omega}\right)\frac{\partial \omega}{\partial x_j}\right] - \frac{\alpha^*\omega}{k}\rho\overline{u_i u_j}\frac{\partial u_j}{\partial x_i} - \beta\rho\omega^2 + 2(1-F_1)\rho\frac{1}{\sigma_{\omega 2}\omega}\frac{\partial k}{\partial x_j}\frac{\partial \omega}{\partial x_j} \quad (11)$$

where $\beta = 0.075$, $\sigma_\omega = 2$, $\sigma_{\omega 2} = 1.168$ and F_1 is the blending function [42].

The spatial discretization for above governing equations uses QUICK scheme and the pressure-velocity coupling method adopts the pressure-based segregated algorithm SIMPLE (Semi-Implicit Method for Pressure-Linked Equations). The entire CFD domain was discretised by over 7.2 million structural mesh cells, prior to which a test for grid independence was done. Refinements of the cell size adjacent to the tower inner wall and in high-gradient regions such as the radiator and nozzles were made through setting the first layer thickness to 7 mm with the aspect ratio no more than 4. A growth rate of 1.05 was then applied to the rest of the cells. A good overall mesh quality was achieved with the maximum orthogonal skewness of 0.33 and the maximum aspect ratio of 8.6. The solutions were taken as converged when all scaled residuals of the dependent variables dropped to the order of 10^{-5} and the additionally monitored variables remained invariable.

2.3. Model validation

As the conceptual air jet-induced swirling plume has not been yet realised on the cooling tower prototype, there is no experimental data available to be used for validation of the CFD results with the swirling plume. However, the results without plume vortex can be compared against existing experimental data of the Gatton NDDCT by setting the simulation conditions same as those of the in-situ measurements.

In the past a few years, a series of tests have been conducted on the Gatton NDDCT including the "constant heat rejection test" [35,40]. In this test, a constant heat was supplied to the cooling tower by an oil fired heater at different ambient temperatures. The air-side and tube-side temperatures of the heat exchangers were measured and then plotted against the ambient temperature. In the CFD model, the same constant heat flux were applied while the atmospheric temperature was varying in the same range. Fig. 3 shows the air exit temperature of the cooling tower obtained from both the experiment and the CFD simulations at a constant heat load of 845 kW with a certain water mass flow under different ambient temperatures. The comparison in the figure indicates a good agreement between both the results suggesting the CFD modelling method is reliable.

3. CFD results on the NDDCT performances with swirling plume

All the 9 cases were simulated by assuming the ambient temperature as 35 °C without the existence of crosswind, and the radiator temperature was fixed at a selected number 51.5 °C while the heat flux was left variable. This condition represents the scenario that the upstream temperature entering the cooling tower is required to be maintained constant. In the following discussions, the air mass flow rate in kg/s and the decreased cooling water temperature (°C) in °C of the heat exchanger are the main metrics used to assess the "cooling performance" of the cooling tower.

The cooling performances of the NDDCT model is firstly assessed for the Cases 0–4, as summarised in Table 2. Here, for convenience, the water temperature change was derived based on assuming a fixed water flow rate in the heat exchanger. The design point of the cooling tower prototype of this model is also listed in the table as a baseline for the comparison. The steady state 3D air streamlines in these five cases are shown in Fig. 4.

The cooling performance enhancement due to the swirling plume is simply observed in the comparison between Case 0 and Case 1. Case 0 reduces the air flow rate by around 14.5% compared with the baseline case simply due to the increase of the ambient temperature from 30 °C to 35 °C. The decreased water temperature reduces following the weakening of the cooling tower's heat dumping capacity, because of not only the smaller flow rate but also a less ITD (initial temperature difference) between the water and the air. However, with the assistance of the air jet-induced swirling plume as Case 1, the air flow rate and consequently the decreased cooling water temperature in the cooling tower is remarkably improved. Specifically, the two indicators are increased compared with those of Case 0 by 52.2% and 38.6%, respectively. The latter is nearly recovered to the design point, i.e. 12.71 °C compared with 12.60 °C. The air jet mass flow rate 16.5 kg/s accounts for only 15.2% of the total airflow in Case 1.

The swirling plume is developed above the air jet nozzle plane in Case 1 as expected, while in the tower space upstream the nozzles, the air flow keeps flowing upward uniformly just as that of Case 0. The tornado-like vortex does remain when the plume leaves the tower outlet although the streamlines gradually become less spiral with the increase of the height. The development of the vortical plume along with the height can be analysed through plotting the plume velocity profiles at different elevations. Fig. 5 depicts the averaged axial and tangential plume velocity components versus radius for the Cases 0–4 at the elevations of y = 5.5 m, 18 m, 20 m, 25 m, 30 m, and 40 m, respectively. The radius was defined as the horizontal distance between a point and the vertical axis of the tower.

Without the induced swirl in Case 0, the axial velocity profile exhibits the expected transition from "top hat" shape to "Gaussian" shape. The momentum flux of the plume above the cooling tower is not conserved because of the presence of buoyancy, and thus the axial velocity increases with height until the plume is fully established [43]. The tangential velocity of the plume is nearly zero everywhere as there is no flow rotation.

Nonetheless, the velocity profiles in Case 1 appear completely different. The tangential velocity profile presents a sharp peak in the near-wall region at the height of 18 m, just above the jet nozzle plane. This suggests that the rotating motion only exists in a ring zone adjacent to the inner tower wall when the plume just encounters the jet. The swirling ratio at this plane is around 6, which is much higher than the ones in [31]. Along with the rise of the plume, the rotation diffuses inward (toward the tower axis) or both inward and outward, while the maximum velocity magnitude decreases. Meanwhile, the position of tangential velocity peak gradually shifts to the tower axis, suggesting an evolution of the original swirl toward an irrotational (free) vortex with a rotational core in the centre. There is a remarkable increase of magnitude in axial velocity profile at the plane of y = 5.5 m comparing Case 1 with Case 0, while both are flat. This directly indicates the air mass flow rate through the heat exchangers in the former is increased without causing any disturbance at this height. The axial velocity profiles at elevations above tower outlet are much wider in Case 1,

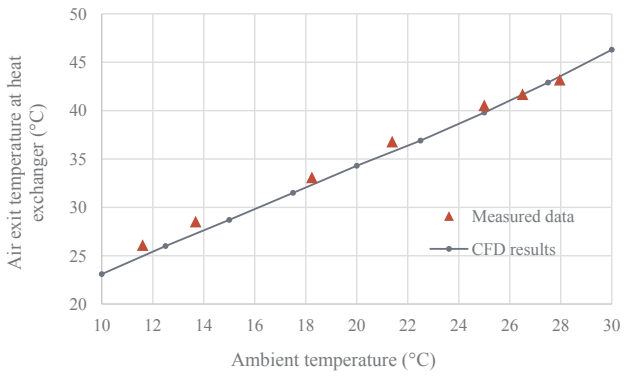

Fig. 3. The experimental and numerical air exit temperature of the cooling tower at an 845 kW heat load.

Table 2
Comparisons in cooling performance among Cases 0, 1, 2, 3, and 4 as well as the baseline.

Parameter	Case 0	Case 1	Case 2	Case 3	Case 4	Design point
Ambient temperature (°C)	35	35	35	35	35	30
Air mass flow rate (kg/s)	71.38	108.69	51.37	73.14	96.153	83.45
Decreased temperature of the cooling water (°C)	9.09	12.60	7.21	9.26	11.42	12.71
Air face velocity at the heat exchanger (m/s)	0.55	0.84	0.40	0.85	0.74	0.64
Air temperature at the heat exchanger exit (°C)	43.22	42.45	41.67	43.08	42.74	39.82
Overall UA based on the face area of the heat exchanger	538.40	758.13	434.64	766.16	679.51	603.89
Total air jet mass flow rate (kg/s)	N/A	16.5	16.5	16.5	16.5	N/A
Percentage changed in flow speed, based on Case 0	N/A	52.3%	−28.0%	2.47%	34.71%	N/A
Percentage increased in heat transfer rate, based on *Case 0*	N/A	38.7%	−20.7%	1.93%	25.7%	N/A
Leverage factor of plume vortex	N/A	2.26	−1.21	0.11	1.50	N/A

which implies that the hot plume out of the cooling tower spreads out more at the same height with the presence of the swirl, which is consistent with the observation in the temperature contours (Fig. 6).

The reason for the increased air flow rate inside the cooling tower may be understood through an examination of the static pressure variations. Fig. 7 shows static pressure contours at the mid-xy plane of the NDDCT model. Fig. 7a suggests that the static pressure inside a cooling tower is always smaller that outside the tower at the same elevation. The difference maximises just above the heat exchanger and fades away along the tower. It is the maximum pressure difference that determines the airflow across the heat exchanger. In pure natural convection case (Case 0), the static pressure difference reduces to zero slightly above the tower outlet. However, with the existence of the plume vortex in Case 1, the negative pressure zone is extended to a considerable height above the tower exit. And, the maximum pressure difference across the heat exchangers is larger than that of Case 0, as if the tower wall is extended further up. Quantitatively, Fig. 8 shows the variations of the static pressure with the elevation from the ground to 70 m for the two cases. The pressure at one elevation was averaged over circular horizontal face with the radius same as the tower's. As seen, Case 1 has a total equivalent draft pressure of 9.0 Pa, almost double of that in Case 0.

For a more comprehensive understanding of the underlying physics, we extended the simulations to three more cases. As mentioned above, Cases 2–4 represent the cases with air jets in radial direction only, in axial direction only, and in both radial and tangential directions, respectively. The air jet speed and flowrate in the 3 cases are all the same as those in Case 1.

According to Figs. 4 and 5, the plume vortex appears only when the jet stream has a tangential component. A jet with only a radial momentum component does not increase the overall airflow in the cooling tower, as verified by Case 2. More precisely, it adversely affects the performance by causing disturbance to the main flow (draft) in the upper part of the cooling tower causing mixing losses only. Consistently, the axial velocity at y = 5.5 m exhibits a lower profile compared to Case 0. In Case 3, on the other hand, the purely vertical air jet results in an increased overall cooling tower airflow. However, the increase is quite minor compared with Case 0. The axial velocity profiles at y = 18 m and 20 m clearly indicate that the main convective airflow of the cooling tower does not significantly benefit from the jet momentum.

Case 4 proves that the jet combining radial and tangential momentum components is also able to enhance the cooling tower performance. In this situation, the air jet is more effective than that of Case 3, but less effective than that of Case 1. It is interesting to note that the axial velocity component at the height slightly above the jet nozzle plane, namely y = 18 m, shows a clear "down draft" near the cooling tower wall. This probably affect the enhancement of the main airflow.

Table 3 lists the cooling performance in Cases 1 and 5–8. Compared with Case 1 as our benchmark, Case 5 bends the jet stream 10° closer to the tower wall, i.e. increase the azimuthal angle a to 70°, while the pitching angle b remains unaltered. This increases the benefit of the vortex. On the contrast, Case 6 is worse than Case 1, which only

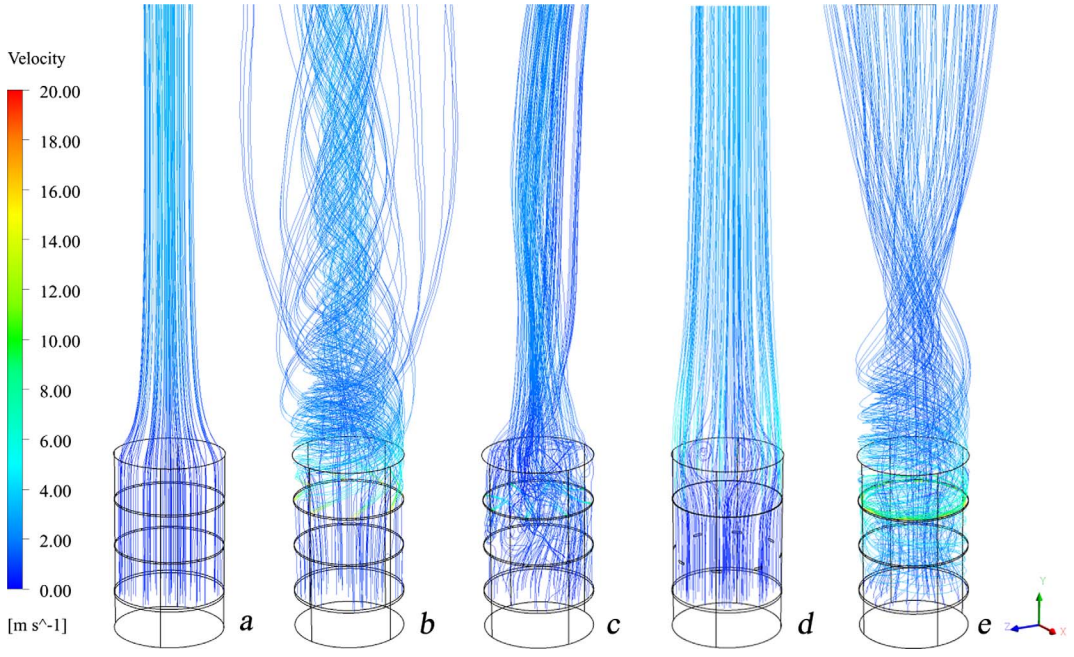

Fig. 4. 3D streamlines starting from the heat exchanger for Case 0 (a), Case 1 (b), Case 2 (C), Case 3 (d) and Case 4 (e).

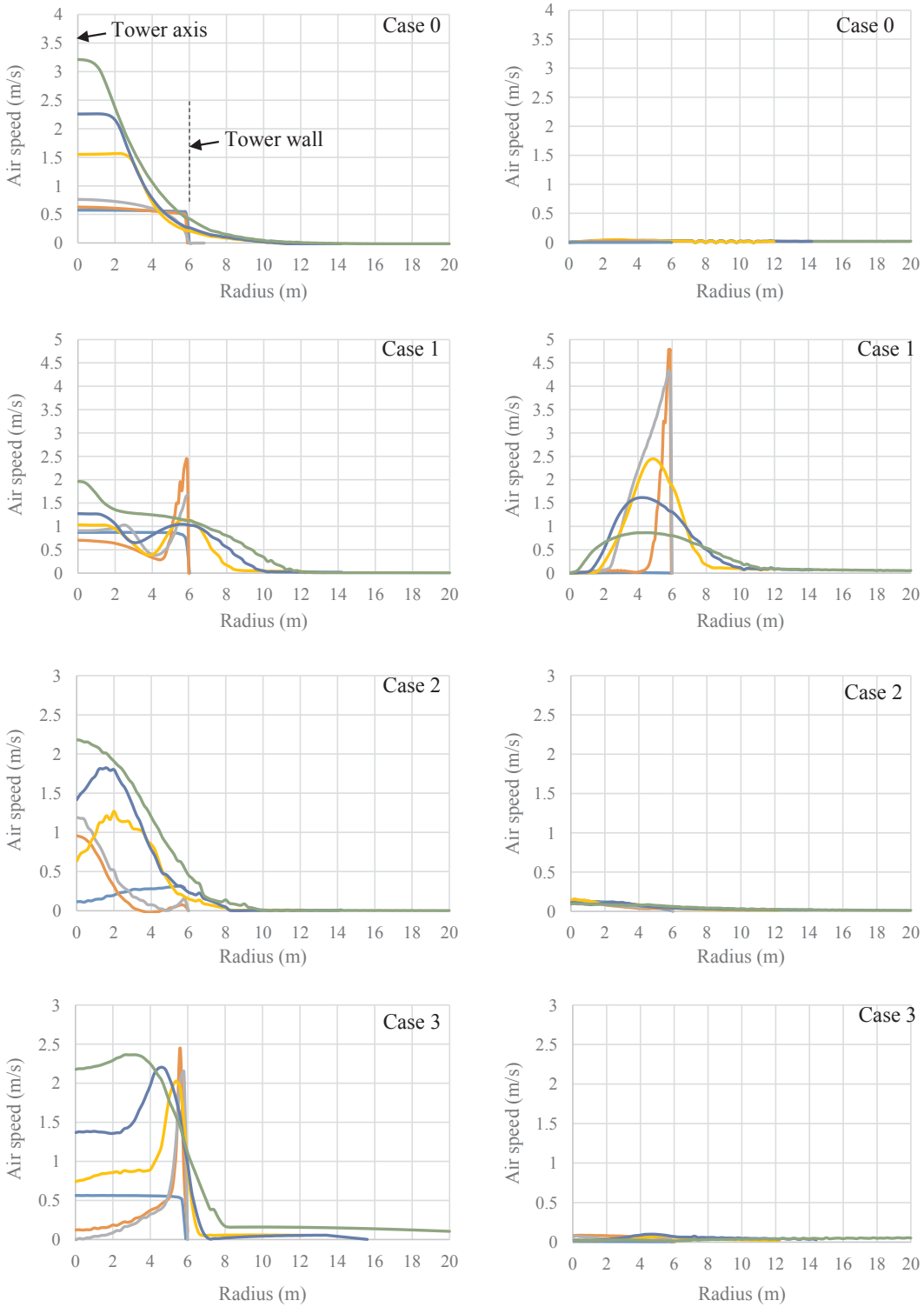

Fig. 5. The averaged axial (left) and tangential (right) velocity components versus the radius for Cases 0–4 at the elevations as indicated in the legend. The origin point of *x*-axis represents the tower axis.

increases the angle *b* to 45°.

Comparisons between Cases 1, 6, 7, and 8 are made to examine whether the jet speed and the normal nozzle area have any effect on the effectiveness of the jet-induced vortex in the cooling tower. This comparison eliminates the influence of the jet direction. Case 7 indicates that reducing the jet speed, compared to that of Case 1 while maintaining the nozzle dimension, results in decreased cooling performance. On the other hand, increasing the nozzle area at the same jet speed (Case 8) will cause a further increase in the total airflow rate through the cooling tower.

In Tables 2 and 3, the leverage factor of vortex is defined as the ratio of the increased overall air mass flow rate based on Case 0 to the total air jet mass flow rate. It indicates the improved air flow rate with inducing air jet for a given configuration. The quantity has a practical meaning as it is related to the overall energy efficiency of the jet-induced vortex system in a NDCT if the jet is generated through fans or

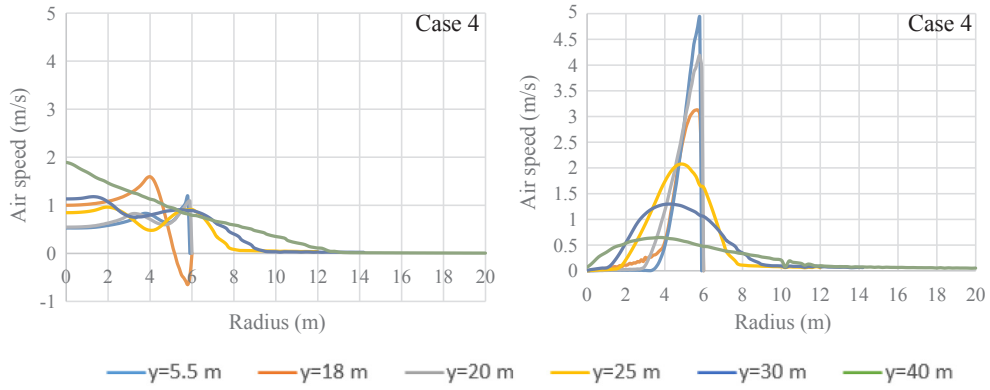

Fig. 5. (*continued*)

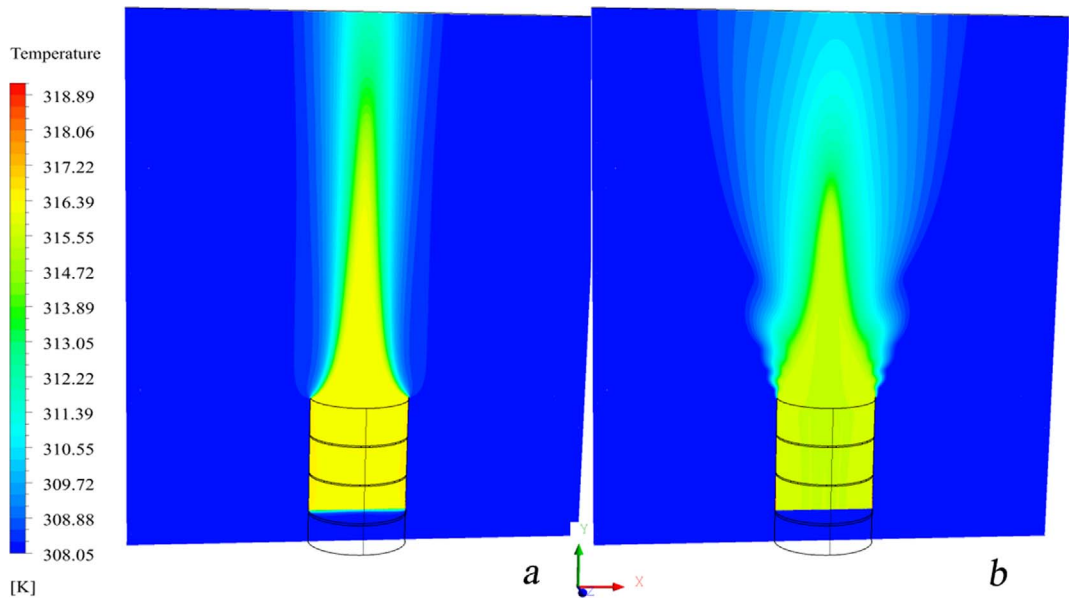

Fig. 6. Temperature contours at the mid-*xy* plane for Case 0 (a) and Case 1 (b).

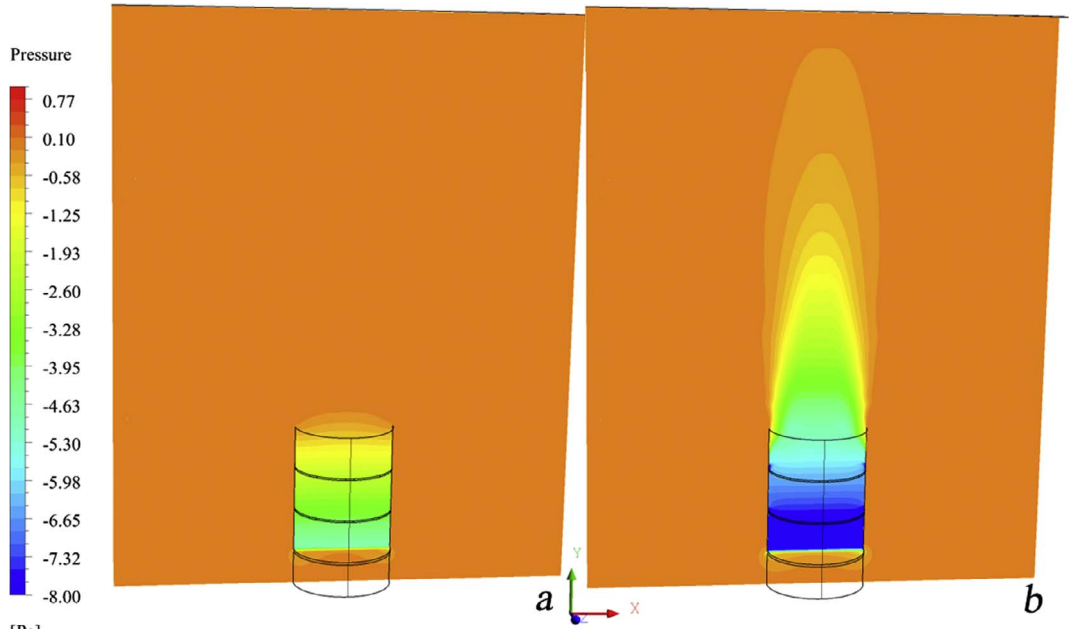

Fig. 7. Static pressure contours at the mid-xy plane in Case 0 and Case 1. For convenience, the static pressure here is redefined as a gauge pressure without consideration of elevation head, namely, by assuming the elevation head zero everywhere.

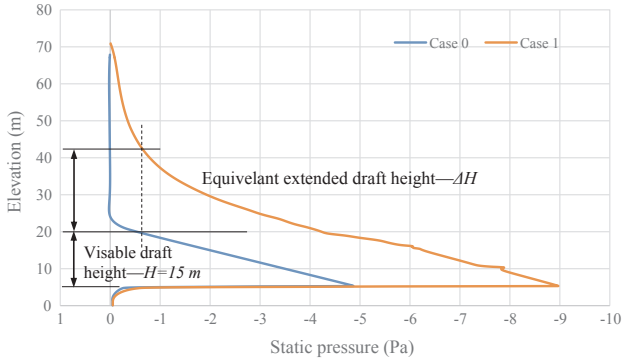

Fig. 8. The mean air static pressure versus the elevation for Cases 0 and 1.

blowers.

4. Analysis and discussions

4.1. A Simplified analytical model for NDDCT performance with swirling plume

The analysis below was carried based the above NDDCT model to explore the mechanism under the airflow enhancement by the swirling plume. Fig. 9 shows an ideal cylindrical NDDCT model with or without air jet nozzles in a 2D view.

In with absence of plume swirl, NDCTs work on the natural convection effect (stack effect): driven by the net buoyancy force, air heated by the heat exchangers is less dense so that it moves upward. Cool air underneath is thus sucked in to replace the hot one, forming a steady-state air flow. If one considers an arbitrary streamline in the cooling tower as shown in Fig. 9, the air accelerates from position 1 at the ground level, overcomes all the resistances in the tower and finally reaches position 2 at the outlet at a speed. In this process, it can be approximated that the mechanical energy along the streamline is conserved, i.e.:

$$P_1 + \frac{1}{2}\rho_1 v_1^2 + \rho_1 g z_1 = P_2 + \frac{1}{2}\rho_2 v_2^2 + \rho_2 g z_2 + \Sigma H_L \tag{12}$$

In Eq. (12), P and z are static pressure and height respectively. ρ_1 and ρ_2 are equivalent to air densities outside and inside the cooling tower, namely ρ_o and ρ_i. ΣH_L denotes the sum of all flow resistances along the flow direction. The elevation at position 1 is zero while the velocity on the streamline, far away from the tower inlet, is negligibly small. If use v_a as the face mean velocity at position 2 instead of v_2, a velocity distribution factor α is introduced, namely $\frac{1}{2}\rho_2 v_2^2 = \alpha\frac{1}{2}\rho_2 v_a^2$. As mentioned above, the mean velocity v_a is the same at any height in the tower between the heat exchanger and the outlet. It is more convenient to express ΣH_L in the form of dynamic pressure of air, i.e. $\Sigma H_L = \frac{1}{2}K\overline{\rho_a} v_a^2$, where K is the pressure loss coefficient between positions 1 and 2, and $\overline{\rho_a}$ is the mean air density between ρ_1 and ρ_2, or ρ_O and ρ_I.

Therefore, Eq. (12) can be rearranged:

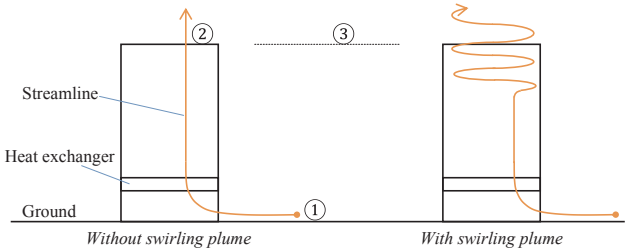

Fig. 9. An ideal model of NDDCT with and without the air jet-induced swirling plume.

$$(P_1 - P_2) - \rho_2 g z_2 = \frac{\alpha}{2}\rho_2 v_a^2 + \frac{1}{2}K\overline{\rho_a} v_a^2 \tag{13}$$

It can be expected that pressure P_2 is slightly smaller than that of the ambient air at same height far away from the cooling tower (position 3), and the small difference is just a dynamic pressure loss due to the airflow exists from the tower outlet [25], i.e.:

$$P_2 = P_3 - \frac{\alpha}{2}K_{to}\rho_2 v_a^2 \tag{14}$$

where K_{to} is the loss coefficient at the tower outlet.

Eq. (14) is then substituted into Eq. (12) to eliminate P_2, which results in three dynamic pressure terms expressed as functions of v_a. These terms can be combined into a single dynamic pressure term $\frac{K+\alpha(1-K_{to})}{2}\overline{\rho_a} v_a^2$. Meanwhile, $(P_1 - P_3)$ is the difference between ambient static pressures at heights 1 and 2, and thus is equal to $\rho_1 g z_2$. Therefore, the following equation can be obtained:

$$\rho_1 g z_2 - \rho_2 g z_2 \cong (\rho_O - \rho_I) g H \cong \frac{K + 1 - K_{to}}{2}\rho_I v_a^2 \tag{15}$$

where H is the cooling tower height which is assumed to approximate to altitude z_2. According to [16], $\alpha \approx 1$ for dry cooling towers where the heat exchangers are arranged horizontally near the tower base.

Eq. (15) can be thought of as the so-called Draft Equation for natural draft cooling towers [25]. As the air flow inside the cooling tower is isentropic and continuous, v_a remains constant anywhere in the above tower model, regardless of the boundary layer at the tower wall. Then, the total air mass flow rate inside the tower, m_a, is expressed as $m_a = \rho_I v_a A$, where A is the cross-section area of the tower.

If one considers the air momentum at the tower outlet face, it can be expressed in a cylindrical coordinate system as

$$\boldsymbol{M} = M_r \hat{\boldsymbol{e}}_{\boldsymbol{r}} + M_\theta \hat{\boldsymbol{e}}_{\boldsymbol{\theta}} + M_z \hat{\boldsymbol{e}}_{\boldsymbol{z}} = m_a \boldsymbol{v} \tag{16}$$

One argues that the momentum in the vertical direction, i.e. z component, is the dominant component and M_z is calculated as:

$$M_z = m_a v_a \cong \frac{2A(\rho_O - \rho_I) g H}{K_\Sigma} \tag{17}$$

Now let us consider the situation when the air jet-induced swirling plume is applied in the cooling tower. As the jet nozzles source the air inside the cooling tower, mass is conserved in the airflow. Similarly, one can select a random streamline through the cooling tower that is

Table 3
The cooling performance comparisons in Cases 1, 5 and 6.

Parameter	Case 1	Case 5	Case 6	Case 7	Case 8
Air mass flow rate (kg/s)	108.69	109.63	93.98	96.55	118.07
Decreased temperature of the cooling water (°C)	12.60	12.66	11.24	11.47	13.47
Air face velocity at the heat exchanger (m/s)	0.84	0.85	0.73	0.75	0.92
Air temperature at the heat exchanger exit (°C)	42.45	42.44	42.68	42.64	42.33
Overall UA based on the face area of the heat exchanger	758.13	766.16	671.82	687.24	823.19
Total air jet mass flow rate (kg/s)	16.5	16.5	16.5	12.4	24.2
Percentage increased in air mass flow, based on *Case 0*	52.27%	53.59%	31.66%	35.26%	65.40%
Percentage increased in heat transfer rate, based on *Case 0*	38.73%	39.19%	23.70%	26.29%	48.31%
Leverage factor of vortex	2.26	2.32	1.37	2.03	1.93

not “sucked in” and “injected out” by any nozzle, although the line should be spiral instead of straight in its upper part as roughly illustrated in Fig. 9. This difference suggests that the overall effect of the introduced jet is to add an extra momentum to the original tower airflow at the nozzle plane. Suppose each jet nozzle injects an airstream inward at a speed v_J, and A_{Jn} is the sum of all nozzle areas—the area perpendicular to jet velocity. The total air jet mass flow rate from all eight nozzles, m_{aJ}, is

$$m_{aJ} = \rho_I v_J A_{Jn} \tag{18}$$

The initial momentum of the jet is then $m_{aJ}\boldsymbol{v_J}$ upon leaving the nozzles with three components in the cylindrical coordinate system written as:

$$\begin{cases} M_{rJ} = v_{rJ} m_{aJ} = m_{aJ}\cos a\cos b\ v_J \\ M_{\theta J} = v_{\theta J} m_{aJ} = m_{aJ}\sin a\cos b\ v_J \\ M_{zJ} = v_{zJ} m_{aJ} = m_{aJ}\sin b\ v_J \end{cases} \tag{19}$$

where v_{rJ}, $v_{\theta J}$ and v_{zJ} are jet speeds in radial, tangential and vertical (axial) directions, as indicated in Fig. 2.

The jet merges with the original airflow in the way which is essentially a mixing of two streams with different speeds. The mixing occurs over a length, away from the nozzles, in which momentum is exchanged. During the transient process, a part of or all initial jet momentum is converted into internal energy, or in other words, simply lost. The remaining jet momentum is then added to the main airflow of the tower, and we can use $\Delta\boldsymbol{M}$ to denote this remaining momentum. Each component of the initial jet momentum in Eq. (19) has a different contribution to $\Delta\boldsymbol{M}$. The radial momentum M_{rJ} causes a tendency of air moving towards the centre, which, obviously, will be quickly lost. The tangential momentum $M_{\theta J}$ causes the air to rotate about the cooling tower axis—a key factor in generating the vortex. The vertical component M_{zJ}, on the other hand, increases the total upward flow momentum. Then, it can be proposed that:

$$\begin{cases} \Delta M_r = 0 \\ \Delta M_\theta = \eta_\theta M_{\theta J} = \eta_\theta v_{\theta J} m_{aJ} \\ \Delta M_z = \eta_z M_{zJ} = \eta_z v_{zJ} m_{aJ} \end{cases} \tag{20}$$

where η_θ and η_z are the proportion factors ranging from 0 to 1 in tangential and vertical directions, respectively. They measure the extent of “non-conservation of momentum” when the jet airstream merges with the cooling tower airflow. They are essentially determined by $v_{\theta j}$ and v_{zj}, respectively, together with A_{jn}.

The airflow in the cooling tower is no longer purely caused by natural draft, but a combination of natural draft and forced convection. Consequently, the original conservation of mechanical energy Eq. (12) is not valid, instead, it should read:

$$P_1 - \left(P_2 + \frac{1}{2}\rho_2 v_z^2 + \frac{1}{2}\rho_2 v_\theta^2 + \rho_2 g z_2\right) = -\frac{\Delta M_\theta + \Delta M_z}{A} + \Sigma H_L \tag{21}$$

Note that all the quantities in the equation such as v_z and v_θ are representing their mean values over the tower cross-section. The term $-\frac{\Delta M_\theta + \Delta M_z}{A}$ on the right hand side is the momentum flux the plume flow obtains from the jet streams and it is an averaged quantity as well.

According to the analysis on the static pressure of the cooling tower with the swirling plume in Figs. 7 and 8, P2 is no longer slightly smaller than P_3. Instead, an additional term should be introduced in Eq. (14) to reflect the extra decrease of the static pressure above the cooling tower outlet resulted by the swirling plume—ΔP:

$$P_2 = P_3 - \frac{\alpha}{2}K_{to}\rho_2 v_z^2 - \Delta P \tag{22}$$

The reason is that, because of the rotational motion of the air about a fixed axis, any element of the flow field is exposed to an outward pressure gradient due to the radial acceleration. As ΔP is expected to be primarily determined by the tangential velocity of the vortex, its value thus can be quantitatively expressed in the form of $\frac{1}{2}\varepsilon\rho_2 v_\theta^2$. Here, ε is a factor relating to the characteristic of the turbulent vortex including v_θ and the swirling ratio [44], which is out of the scope of this paper.

Now combine Eqs. (15) and (19)–(22). Also, note that the terms $-\frac{\Delta M_\theta}{A}$ and $-\frac{1}{2}\rho_2 v_\theta^2$ on each side of Eq. (21) can cancel out as the dynamic pressure due to the tangential velocity is only caused by the tangential momentum flux of the jet the plume obtains, but this does not mean the plume’s angular (tangential) momentum disappears. We can now drive the modified Draft Equation below:

$$(\rho_O - \rho_I)gH + \eta_z v_{zJ}\frac{\rho_I v_J A_{Jn}}{A} + \frac{\varepsilon}{2}\rho_2 v_\theta^2 \cong \frac{K + 1 - K_{to}}{2}\rho_I v_z^2 \tag{23}$$

The right hand side of the equation remains similar to the one of Eq. (15). The additional terms on the left hand side suggests that, when the swirling plume is generated by the air jet in a natural draft cooling tower, the increase in the “draft” (i.e. the left hand side of the Draft Equation) is attributed to two effects: the vertical momentum flux of the jet the plume flow absorbs, namely the terms $\eta_z v_{zJ}\frac{\rho_I v_J A_{Jn}}{A}$, and the extra pressure change above the cooling tower outlet caused by plume vortex $\frac{\varepsilon}{2}\rho_2 v_\theta^2$. The former directly influences the airflow’s dynamic pressure, while the latter augments the static pressure though it is expressed in a dynamic-pressure form. However, this change in static pressure is essentially related to the tangential momentum flux of the jet, namely $-\frac{\Delta M_\theta}{A}$.

It is the increase of the left hand side that causes the overall upward air flow rate v_z to increase on the other side of Eq. (23). The above comparisons in the CFD results for Cases 1–4 suggest that the tangential momentum of the air jet is a dominant factor in improving the cooling tower performance, as the pure vertical air jet increase the tower flow rate only a little. This can be explained as that between the two extra terms in Eq. (23), $\frac{\varepsilon}{2}\rho_2 v_\theta^2$ is probably much larger.

The angular momentum of the swirling plume upon leaving the tower outlet plane has a tendency to conserve. However, because of the viscous resistance of the surrounding air, the momentum gradually dissipates at some distance above the cooling tower. This leaves a physical meaning for the aforementioned equivalent extended cooling tower draft height ΔH. Mathematically, Eq. (23) can be simplified and rearranged to the following form

$$(\rho_O - \rho_I)g(H + \Delta H) \cong \frac{K + 1 - K_{to}}{2}\rho_I v_z^2 \tag{24}$$

where the invisible extended tower height ΔH is derived from the two additional terms of Eq. (23). For convenience, we may simply write ΔH as a function of the air jet characteristic parameters, i.e. $\Delta H = f(\eta_z, v_{zJ}, A_{Jn}, v_J, \varepsilon)$ or even $\Delta H = f(a, b, v_J, A_{Jn})$, by assuming the factor ε is also a function of the air jet characteristic parameters.

Therefore, the improvement in the draft of the NDDCT is determined by the jet speed, direction, and the jet nozzle size. This argument is supported by the CFD result comparison of Case 1 with Cases 5–8. For instances, increasing angle a from 60° to 70° while keep the angle b fixed at 30° has a better outcome, because the tangential momentum of the jet $M_{\theta J} = m_{aJ}\sin a\cos b v_J$ is increased. However, increasing angle b from 30° to 45° while keep the angle b adversely affects ΔH, as it increases M_{zJ} but decreases $M_{\theta J}$. This further supports the claim that the jet tangential momentum that the swirling plume flow absorbs is a critical factor. Furthermore, the jet mass flow rate is positively related to ΔH.

4.2. Energy consumption of the air jet-induced swirling plume in NDDCT

In this section, the power consumed on the NDDCT with air jet-induced swirling plume in configuration of Case 5, the best case, is estimated and compared against that of a conventional fan-forced cooling tower/cooler with a same cooling capacity. The calculation of fan power is based on basic fan theories and some simplified assumptions.

The mechanical cooling tower is assumed to use exactly the same horizontally-arranged heat exchanger bundles and two fans with a typical diameter of 3.4 m [45] above the bundles instead of the 15 m-tall tower shell. The fans provide an identical air flow rate through the heat exchangers under the same ambient condition as in Case 5.

By theory, the shaft power input W_F to fans or blowers is calculated through total efficiency η_{Ft}, i.e.

$$W_F = \frac{V_F \Delta P_{Ft}}{\eta_{Ft}} \tag{26}$$

where V_F and ΔP_{Ft} are the volumetric flow rate and total pressure of the fan, respectively. According to the definition of fan total pressure, one has:

$$V_F \Delta P_{Ft} = V_F \left(\Delta P_{Fs} + \frac{1}{2}\rho_a v_F^2 \right) = \Delta P_{Fs} V_F + \frac{1}{2} m_a v_F^2 \tag{27}$$

where ΔP_{Fs} is the static pressure of the fan, and v_F is the air speed at the fan exit. It is difficult to estimate the static pressure of a single fan without knowing specific fan characteristics. However, in a fan system, the pressure is always determined by the total pressure resistance throughout the system. According to Table 2, the air flow rate and the pressure drop across the heat exchangers are maintained at 109.63 kg/s and 9.0 Pa, respectively. If we ignore all the pressure resistances other than the one due to the heat exchangers [34], the useful work done by the fans consists of the pressure energy that is used to overcome the pressure resistance of the heat exchangers and the kinetic energy at the two fan exits. Therefore, Eq. (27) becomes:

$$V_F \Delta P_{Ft} = \frac{\Delta P_r m_a}{\rho_a} + m_{aF} v_{aF}^2 = 9.0 \times \frac{109.63}{1.145} + \frac{109.63}{2} \times \left(\frac{109.63/2}{1.145 \times \pi \times (3.4/2)^2} \right)^2 = 2.39 \text{ kW} \tag{28}$$

where m_{aF} and v_{aF} are the air mass flow rate and the speed in a single fan. Then, the power consumption of the fans is

$$W_F = \frac{2.39}{\eta_{Ft}} \text{ kW} \tag{29}$$

On the other hand, for the air jet nozzles, the fans or blowers used in the nozzles are assumed to work without any obstructions in order to keep the comparison fair. The pressure loss due to the fans themselves and ducts as well as nozzles are usually quite small and thus are also ignored here. Therefore, the air kinetic energy is the only useful work. The power consumption is then

$$W_J = \frac{\frac{1}{2} m_a v_j^2}{\eta_{Ft}} = \frac{\frac{1}{2} \times 16.5 \times 20^2}{\eta_{Ft}} = \frac{3.30}{\eta_{Ft}} \text{ kW} \tag{30}$$

Obviously, the two power consumptions in Eqs. (29) and (30) rely on the total fan efficiencies. Now, if we assume these efficiencies are same, for example 80%, the total powers consumed in the vortex-enhanced NDDCT and the fan-induced cooling tower are 4.1 kW and 3.0 kW, respectively.

Although the power consumption in jet-induced swirling plume NDCCT is higher, the two are still comparable. However, the huge advantage of the former over the latter lies in life-long services. This is because the vortex enhancement is in operation for short-term only. The nozzle jet is only turned on in a small part of time over a year when the ambient temperature is too high for the NDDCT to perform as designed; whereas the fan-based cooling tower relies on fans running all the time.

4.3. Effect of the swirling plume cooling tower on energy performance of power cycle

The prototype of the 20 m-tall NDDCT model was designed for an expected supercritical CO_2 cycle-based small CST power plant (up to 1 MWe) [34]. Therefore, the enhancement of the heat dumping capacity in the cooling tower with the proposed air jet-induced swirling plume can be evaluated, coupled with a performance calculation of an entire power conversion cycle for the CST plant [46].

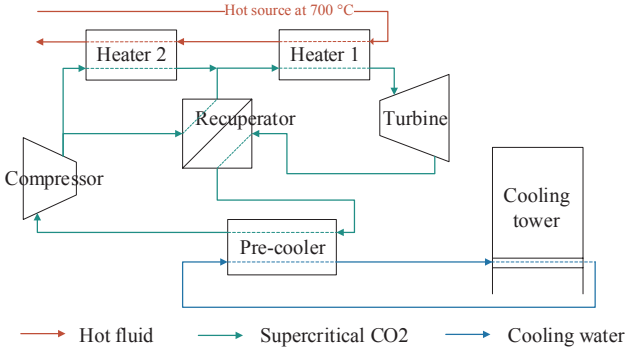

Fig. 10. A schematic drawing of the split recuperated sCO_2 Brayton cycle indirectly cooled by the NDDCT with swirling plume.

In this study, a modelling methodology similar to the ones introduced in [35] was adopted to establish a split recuperated supercritical CO_2 (sCO_2) Brayton cycle model, with all the components illustrated in Fig. 10. Assumptions were made to some of the key component parameters as constraints or initial conditions of the cycle model, as shown in Table 4. By adjusting the flow rates of the sCO_2 and hot source fluid, the cycle output a net power of 548.9 kWe with the cool end (cooling tower) performance matching the result in the design point, i.e. the decreased cooling water temperature of 12.7 °C at the flow rate of 15.5 kg/s and the ambient temperature of 30 °C.

With the hot source flow rate fixed, the temperature of the returning water from the cooling tower was varied as per the cooling performances derived from the results of Cases 1–9. Meanwhile, the cooling water mass flow rate was also adjusted to maintain a constant temperature of the water leaving the pre-cooler, which was consistent with the boundary condition of the aforementioned CFD heat exchanger model. The temperature changes in the cooling water resulted in a series of consequent temperature and pressure changes within the cycle so that the net power output varied accordingly. Fig. 11 depicts the net power output of the cycle for the design point and in Cases 0, 1, and 5.

The figure shows that the increase of the ambient temperature from 30 °C (Design point) to 35 °C (Case 0) causes the net power output to drop by 27.3 kWe, or 4.98%. In Cases 1 and 5, the cooling performance of the NDDCT is enhanced by the jet-induced swirling plume at the higher ambient temperature. As a result, their cycle power outputs recover to the level nearly same as that of the design point. The energy consumption of the jet for Cases 1 and 5, on the other hand, is much smaller than the regained power output—around 1/7, according to the estimation in the previous section.

The overall energy performance of the swirling plume cooling tower on the power cycle can be embodied in the consideration for long-term operation, e.g. one year period. Suppose the time when ambient

Table 4
Key component parameters in the sCO_2 power cycle model.

Component parameter	Value
Heat source fluid temperature	700 °C
Turbine pressure ratio	3.1
Compressor inlet/outlet pressure @ design point	6.43 MPa/20 MPa
Turbine efficiency	85%
Compressor efficiency	80%
Pressure loss at each heat exchanger	3%
Pinch point temperature difference at the recuperator	5 °C
Cooling water outlet temperature leaving the pre-cooler	51.5 °C
Heat exchange area of the pre-cooler	40 m^2

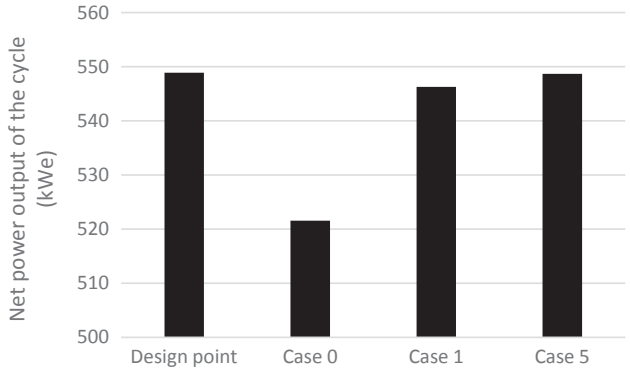

Fig. 11. The net power output of the cycle for the design point and in Cases 0, 1, and 5.

temperate is above the designed 30 °C accounts for 5% of a year, and the average temperate for this period is 35 °C. For the above supercritical CO_2-based Brayton cycle, the swirling plume concept would help to recover a net total of 10,088 kWh output electricity, compared to the cycle with a normal 20 m-tall NDDCT. If the aforementioned mechanical cooling tower/cooler is taken into the comparison, this concept would save roughly 24,500 kWh parasitic electricity, by assuming the fan power is fixed at 3.0 kW all the time.

5. Conclusions

The heat dump performance of natural draft cooling towers (NDCTs) is one of the crucial factors affecting the overall power conversion (heat-to-electricity) efficiency in concentrated solar or coal-fired thermal power plants. To boost the energy efficiency of these power plants, a new concept of cooling performance enhancement in NDCTs against high ambient temperatures has been proposed by the authors. The basic idea of the concept is to create high-swirling ratio plume vortex in and above the towers by introducing a number of blower-powered air jets at certain locations.

In this paper, using a 20 m-tall natural draft dry cooling tower (NDDCT) model, the effectiveness of the conceptual method on the cooling enhancement has been verified numerically and its working mechanism has been initiatorily analysed. The benefit of using such a swirling plume NDDCT to power cycles as well as its power consumption have been investigated through simplified analytical models. The study comes to the following conclusions.

1. The jet-induced swirling plume is able to improve the cooling performance of NDCTs. Through numerical modelling, we found that the proposed plume vortex enhances the total air flow rate and the decreased cooling water temperature of the 20 m-tall NDDCT by at least 53.6% and 3.57 °C (39.3%) respectively, at 35 °C ambient temperature. The enhancement enables the cooling tower recover its performance to the level nearly same to that at 30 °C ambient temperature.
2. The swirling plume NDDCT increases the net power output of a half megawatt-scale sCO_2-based CST power cycle by 4.98% at the atmospheric temperature of 35 °C. The energy consumption for creating such a benefit only accounts for around 1/7 of the regained electricity.
3. The concept works for the reason that the swirling plume creates an equivalent extra draft height on top of the tower, ΔH, which is attributed to two vortical effects. ΔH is then proposed to be functionally related to the air jet speed, the direction (both the azimuthal pitching angles), and the nozzle size. The study compared 9 combination cases of the above parameters, and found that the angular momentum of the swirling plume is the critical factor in determining the effect of the swirling plume.

The findings of the study point out that the jet-induced swirling plume concept is potentially feasible in real applications on natural draft cooling towers, either wet- or dry-type, to recover their cooling capacity at high ambient temperatures. Although the power drawn by the system is still comparable to that of a fan-forced cooler working under the exactly same condition, the system would run only during temperature extremes. Overall, the additional energy usage is relatively small, leading to a low average power consumption. Besides, the method has no influence to the NDCTs in normal pure natural convection operations.

By identifying the critical factor in the vortex effects and introducing the leverage factor, the work suggest that, for a given NDCT, there exists optimal combination/s among the air jet speed, direction and the nozzle size. Other influencing parameters may also exist, including the location of the air jets.

Acknowledgements

This research was performed as part of the Australian Solar Thermal Research Initiative (ASTRI), a project supported by the Australian Government, through the Australian Renewable Energy Agency (ARENA).

References

[1] Boulay RB, Cerha MJ, Massoudi M. Dry and hybrid condenser cooling design to maximize operating income. In: ASME 2005 Power Conference, ASME, Chicago, Illinois, USA; 2005. p. 167–75.
[2] Stabat P, Marchio D. Simplified model for indirect-contact evaporative cooling-tower behaviour. Appl Energy 2004;78:433–51.
[3] Fisenko SP, Brin AA, Petruchik AI. Evaporative cooling of water in a mechanical draft cooling tower. Int J Heat Mass Transf 2004;47:165–77.
[4] Fisenko SP, Petruchik AI, Solodukhin AD. Evaporative cooling of water in a natural draft cooling tower. Int J Heat Mass Transf 2002;45:4683–94.
[5] He S, Guan Z, Gurgenci H, Hooman K, Lu Y, Alkhedhair AM. Experimental study of film media used for evaporative pre-cooling of air. Energy Convers Manage 2014;87:874–84.
[6] Sun Y, Guan Z, Gurgenci H, Hooman K, Li X, Xia L. Investigation on the influence of injection direction on the spray cooling performance in natural draft dry cooling tower. Int J Heat Mass Transf 2017;110:113–31.
[7] Alkhedhair A, Jahn I, Gurgenci H, Guan Z, He S, Lu Y. Numerical simulation of water spray in natural draft dry cooling towers with a new nozzle representation approach. Appl Therm Eng 2016;98:924–35.
[8] Eugene Grindle JC. Roger Lawson improving natural draft cooling tower performance with heat injection. In: 2002 International Joint Power Generation Conference, ASME, Scottsdale, Arizona, USA; 2002.
[9] Zou Z, Guan Z, Gurgenci H, Lu Y. Solar enhanced natural draft dry cooling tower for geothermal power applications. Sol Energy 2012;86:2686–94.
[10] Smrekar J, Oman J, Širok B. Improving the efficiency of natural draft cooling towers. Energy Convers Manage 2006;47:1086–100.
[11] Li X, Xia L, Gurgenci H, Guan Z. Performance enhancement for the natural draft dry cooling tower under crosswind condition by optimizing the water distribution. Int J Heat Mass Transf 2017;107:271–80.
[12] Zhao Y, Long G, Sun F, Li Y, Zhang C, Liu J. Effect mechanism of air deflectors on the cooling performance of dry cooling tower with vertical delta radiators under crosswind. Energy Convers Manage 2015;93:321–31.
[13] Zhao Y, Sun F, Li Y, Long G, Yang Z. Numerical study on the cooling performance of natural draft dry cooling tower with vertical delta radiators under constant heat load. Appl Energy 2015;149:225–37.
[14] Zhao YB, Long G, Sun F, Li Y, Zhang C. Numerical study on the cooling performance of dry cooling tower with vertical two-pass column radiators under crosswind. Appl Therm Eng 2015;75:1106–17.
[15] Goodarzi M, Ramezanpour R. Alternative geometry for cylindrical natural draft cooling tower with higher cooling efficiency under crosswind condition. Energy Convers Manage 2014;77:243–9.
[16] Wang W, Zhang H, Liu P, Li Z, Lv J, Ni W. The cooling performance of a natural draft dry cooling tower under crosswind and an enclosure approach to cooling efficiency enhancement. Appl Energy 2017;186:336–46.
[17] Wang W, Lyu J, Zhang H, Liu Q, Yue G, Ni W. A performance enhancement of a natural draft dry cooling tower in crosswind via inlet flow field reconstruction. Energy Build 2018;164:121–30.
[18] Ma H, Si F, Kong Y, Zhu K, Yan W. Wind-break walls with optimized setting angles for natural draft dry cooling tower with vertical radiators. Appl Therm Eng 2017;112:326–39.
[19] Wang Q, Zhu J, Lu X. Numerical simulation of heat transfer process in solar enhanced natural draft dry cooling tower with radiation model. Appl Therm Eng 2017;114:977–83.
[20] Kong Y, Wang W, Yang L, Du X, Yang Y. A novel natural draft dry cooling system

with bilaterally arranged air-cooled heat exchanger. Int J Therm Sci 2017;112:318–34.
[21] Chen L, Yang L, Du X, Yang Y. Performance improvement of natural draft dry cooling system by interior and exterior windbreaker configurations. Int J Heat Mass Transf 2016;96:42–63.
[22] Alavi SR, Rahmati M. Experimental investigation on thermal performance of natural draft wet cooling towers employing an innovative wind-creator setup. Energy Convers Manage 2016;122:504–14.
[23] Liao HT, Yang LJ, Wu XP, Du XZ, Yang YP. Impacts of tower spacing on thermo-flow characteristics of natural draft dry cooling system. Int J Therm Sci 2016;102:168–84.
[24] Moore FK. On the minimum size of large dry cooling towers with combined mechanical and natural draft. J Heat Transf 1973;95:383–9.
[25] Kroger DG. Air-cooled heat exchangers and cooling towers. Tulsa, Okl, USA: Pennwell Corp; 2004.
[26] Gasparini G, Barbieri G. Performance augmentation of natural draft cooling towers. In: Google Patents; 2006.
[27] Bosman P. Fan-assisted wet coolong tower and method of reducing liquid loss. In: Google Patents; 2005.
[28] Schreiber H. Fan cooling tower design and method. In: Google Patents; 2014.
[29] Gerald RAW, Stillman I. Confined Vortex Cooling Tower, in USA; 1983.
[30] McAllister Jr JE, Aiken SC. Vortex-augmented cooling tower-windmill combination, in, the United States Department of Energy, Washington, D.C., USA; 1985.
[31] Kashania MMH, Dobregob KV. Heat and mass transfer in the over-shower zone of a cooling tower with flow rotation. J Eng Phys Thermophys 2013;86:1490–9.
[32] Kashani MMH, Dobrego KV. Influence of flow rotation within a cooling tower on the aerodynamic interaction with crosswind flow. J Eng Phys Thermophys 2014;87:385–93.
[33] Dobrego KV, Davydenko VF, Koznacheev IA. Use of oriented spray nozzles to set the vapor-air flow in rotary motion in the superspray space of the evaporative chimney-type tower. J Eng Phys Thermophys 2016;89:157–66.
[34] Li X, Guan Z, Gurgenci H, Lu Y, He S. Simulation of the UQ Gatton natural draft dry cooling tower. Appl Therm Eng 2016;105:1013–20.
[35] Li X, Duniam S, Gurgenci H, Guan Z, Veeraragavan A. Full scale experimental study of a small natural draft dry cooling tower for concentrating solar thermal power plant. Appl Energy 2017;193:15–27.
[36] Lu Y, Gurgenci H, Guan Z, He S. The influence of windbreak wall orientation on the cooling performance of small natural draft dry cooling towers. Int J Heat Mass Transf 2014;79:1059–69.
[37] Lu Y, Guan Z, Gurgenci H, Alkhedhair A, He S. Experimental investigation into the positive effects of a tri-blade-like windbreak wall on small size natural draft dry cooling towers. Appl Therm Eng 2016;105:1000–12.
[38] Lu Y, Guan Z, Gurgenci H, Zou Z. Windbreak walls reverse the negative effect of crosswind in short natural draft dry cooling towers into a performance enhancement. Int J Heat Mass Transf 2013;63:162–70.
[39] Lu Y, Guan Z, Gurgenci H, Hooman K, He S, Bharathan D. Experimental study of crosswind effects on the performance of small cylindrical natural draft dry cooling towers. Energy Convers Manage 2015;91:238–48.
[40] Li X, Gurgenci H, Guan Z, Wang X, Duniam S. Measurements of crosswind influence on a natural draft dry cooling tower for a solar thermal power plant. Appl Energy 2017;206:1169–83.
[41] Meyyappan M, Schwarz M, Perry J. Modelling of swirl jet flows. In: 1st International Conference on CFD in the Mineral & Metal Processing and Power Generation Industries, Melbourne, Australia; 1997.
[42] A. Inc., FLUENT User's Guide, vol. 2011, ANSYS Inc., New Hampshire, USA, 2011.
[43] Henderson-Sellers B. The zone of flow establishment for plumes with significant buoyancy. Appl Math Model 1983;7:395–8.
[44] Klimenko AY. Strong swirl approximation and intensive vortices in the atmosphere. J Fluid Mech 2014;738:268–98.
[45] Lu Y, Guan Z, Hooman K, Parulekar PS. An investigation on cooling performance of air-cooled heat exchangers used in coal seam gas production. Heat Transf. Eng 2016.
[46] Deng H, Boehm RF. An estimation of the performance limits and improvement of dry cooling on trough solar thermal plants. Appl Energy 2011;88:216–23.